PHOTOSYNTHETICA 38 (4): 581-599, 2000

Fluorescence lifetime imaging (FLI) in real-time – a new technique in photosynthesis research

O. HOLUB*, M.J. SEUFFERHELD**, C. GOHLKE*, GOVINDJEE**, and R.M. CLEGG*,+

*Department of Physics, Laboratory for Fluorescence Dynamics, University of Illinois at Urbana-Champaign, 1110 West Green St., Urbana, IL 61801, USA**
*Department of Plant Biology, 265 Morrill Hall, University of Illinois at Urbana-Champaign, 505 S Goodwin Ave., Urbana, IL 61801, USA***

Abstract

We describe an instrument that allows the rapid measurement of fluorescence lifetime-resolved images of leaves as well as sub-cellular structures of intact plants or single cells of algae. Lifetime and intensity fluorescence images can be acquired and displayed in real time (up to 55 lifetime-resolved images per s). Our imaging technique therefore allows rapid measurements that are necessary to determine the fluorescence lifetimes at the maximum (P level) fluorescence following initial illumination during the chlorophyll (Chl) *a* fluorescence transient (induction) in photosynthetic organisms. We demonstrate the application of this new instrument and methodology to measurements of: (*1*) *Arabidopsis thaliana* leaves showing the effect of dehydration on the fluorescence lifetime images; (*2*) *Zea mays* leaves showing differences in the fluorescence lifetimes due to differences in the bundle sheath cells (having a higher amount of low yield photosystem 1) and the mesophyll cells (having a higher amount of high yield photosystem 2); and (*3*) single cells of wild type *Chlamydomonas reinhardtii* and its non-photochemical quenching mutant NPQ2 (where the conversion of zeaxanthin to violaxanthin is blocked), with NPQ2 showing lowered lifetime of Chl *a* fluorescence. In addition to the lifetime differences referred to in (*1*) and (*2*), structural dependent heterogeneities in the fluorescence lifetimes were generally observed when imaging mesophyll cells in leaves.

Additional key words: *Arabidopsis*; *Chlamydomonas*; FLIM; frequency domain; homodyne; microscopy; modulation; phase; photosystems 1 and 2; stress; time domain; *Zea*.

Received 31 October 2000, *accepted* 20 March 2001.
+Corresponding author; e-mail: rclegg@uiuc.edu

Abbreviations: A, absorption cross section; AC, amplitude of the alternating part of the modulated radiation; AOM, acousto-optical modulator; CCD, charge-coupled device; Chl, chlorophyll; Chl a^*, excited state of Chl *a*; CP29, a 29 kDa minor Chl-protein complex; CW, continuous wave; DC, amplitude of the direct part of the modulated radiation; DCMU, 3-(3,4-dichlorophenyl)-1,1-dimethylurea; $\Delta\varphi$, phase difference between φ_{mcp} and φ_{ex}; F, fluorescence intensity; DF, depth of focus; f_{ex}, frequency of the modulated excitation radiation; FLI, fluorescence lifetime-resolved imaging; FLIM, fluorescence lifetime-resolved imaging microscopy; F_{max}, maximum fluorescence level; F_P, relative maximum (P, peak) of a fluorescence transient curve; F_0, initial minimum fluorescence level; f_1, fractional intensity of the first lifetime component in a two lifetime component system; f_2, fractional intensity of the second lifetime component in a two lifetime component system; φ, phase of a fluorophore, the phase difference between φ_{em} and φ_{ex}; φ_{em}, phase of the modulated emission radiation; φ_{ex}, phase of the modulated excitation radiation; φ_{mcp}, phase of the image intensifier modulation; Φ, quantum yield of fluorescence; GPIB, general purpose interface bus; HF, high frequency; HS, high salt; I, irradiance by excitation radiation; LASER, light amplification by stimulated emission of radiation; LHC2b, the major light-harvesting-complex of PS2; M, modulation; M_{em}, modulation depth of the emission radiation; M_{ex}, modulation depth of the excitation radiation; MB, mega byte; MCP, microchannel plate; NA, numerical aperture; NPQ, non-photochemical quenching; OJIPSMT, nomenclature of transient curve (O origin, J inflection, I intermediary hump, P peak, S quasi-steady state, M relative maximum, T terminal steady state); PC, personal computer; PCI, peripheral component interconnect, computer local bus standard; PS, photosystem; PS2RC, reaction center of PS2; psbS gene product, a 22 kDa protein involved in non-photochemical quenching phenomenon; q_P, photochemical quenching; RAM, random access memory; RF, radio frequency; RS 232, recommended standard (RS) interface for connecting serial devices; TAP, tris-acetate phosphate; τ, lifetime of fluorescence; τ_{mod}, apparent single lifetime calculated from modulation; τ_{phase}, apparent single lifetime calculated from phase; τ_0, intrinsic lifetime of fluorescence; τ_1, first lifetime component of two lifetime component system; τ_2, second lifetime component of two lifetime component system; $\langle\tau\rangle$, average lifetime of fluorescence; W_{dist}, working distance; WT, wild type; ω, radial frequency of the modulated radiation.

Acknowledgements: We thank Martin Hohmann-Marriott for discussions, Krishna K. Niyogi for the seeds of the NPQ mutants, and John M. Cheeseman for support. The work was supported by the Integrated Photosynthesis Training Grant from the NSF, DBI 96-02240 and NIH, PHS 5 P41 RRO3155.

Introduction

The responses of the photosynthetic apparatus to environmental and biotic stresses are spatially, as well as temporally, heterogeneous. This heterogeneity presents a constant challenge for understanding changes in photosynthesis performance due to anthropogenic as well as biological stress. These changes are technically difficult to study and interpret. In recent years numerous techniques have been developed for detecting differential performance of photosynthesis (cf. Kramer and Crofts 1996). Imaging techniques have been applied broadly for screening mutants (Niyogi *et al.* 1997), studying plant responses to abiotic stress (Oxborough and Baker 1997), mapping spatial distributions of leaf photosynthesis (Genty and Meyer 1995), diagnosing diseases (Daley 1995, Scholes and Rolfe 1996), and studying UV protection in crops (Mazza *et al.* 2000). Fluorescence intensity imaging has been applied for studying the processes involved in post-harvest physiology (DeEll and Toivonen 2000, Ciscato 2000) and predicting seed quality (Jalink *et al.* 1998). For a review on fluorescence imaging in plants see Buschmann and Lichtenthaler (1998).

About a decade ago several independent groups developed fluorescence lifetime-resolved imaging, FLI, systems (for reviews see Wang *et al.* 1992, Clegg *et al.* 1996, Gadella 1999). These developments became possible as soon as electronic devices such as charge-coupled device (CCD) cameras, high-speed gated image intensifiers, and the necessary high performance computers became easily available.

Many of these methods require long times (15-30 min) for data acquisition and analysis. For medical diagnostic imaging and for applications in biology such long measurement times are often not acceptable. Many biological processes operate on a much faster time scale than this; in addition, sample movements or photobleaching make rapid measurements essential. For this reason, we have developed a FLI instrument that can acquire, analyze, and display lifetime-resolved images in real-time [see Schneider and Clegg (1997) for details]. Here we describe major improvements in this instrumentation, and show how such a real-time frequency-domain FLI instrument can be applied in plant science and studies of photosynthesis in leaves and algae; it can be equally applied to cyanobacteria and prochlorophytes.

Chlorophyll (Chl) *a* fluorescence is an intrinsic, noninvasive, nondestructive, and highly sensitive probe of the photosynthetic performance of photosystem (PS) 2, as well as the entire photosynthetic apparatus (Govindjee *et al.* 1986, Karukstis 1991, Govindjee 1995, Papageorgiou 1996). The fluorescence intensity of PS2 is 5-10 times higher than the fluorescence intensity of PS1. Almost all the variable Chl *a* fluorescence originates in PS2 [see Byrdin *et al.* (2000) for discussion of a small variable fluorescence in PS1]. Steady-state measurements of the Chl *a* fluorescence yield have provided extensive information on photosynthesis. However, the fluorescence from Chl *a* is difficult to interpret because the excited state of Chl *a* (Chl a^*) is subjected to a number of non-radiative de-excitation routes (heat, energy transfer, and photochemical trapping) that compete with fluorescence emission. Because of this kinetic competition, changes in the probability of de-excitation by one or more of the non-radiative pathways alter the overall fluorescence yield of Chl a^*. Variations in the fluorescence yield *in vivo* are mainly the result of two major processes: photochemical quenching (q_P) and a group of processes called non-photochemical quenching, NPQ (Gilmore and Govindjee 1999, Samson *et al.* 1999). Chl *a* fluorescence intensity (F) measurements alone at constant incident excitation irradiance (I) cannot distinguish changes in the cross section for absorption (A) of the fluorescent PS2 antenna from changes in the quantum yield of fluorescence (Φ): $F = \Phi\ I\ A$. However, the lifetime of fluorescence (τ) measures Φ directly: $\tau = \tau_0\ \Phi$ (where τ_0 is the intrinsic or natural lifetime of fluorescence, describing the case in which the fluorescence is the only de-excitation pathway).

The average time an excited molecule remains in excited state is determined by the number of de-activation pathways and their competing rates. Dynamic information about complex photosynthetic processes can be obtained using lifetime-resolved fluorescence measurements to determine the rates of de-activation from the excited state of Chl *a*. Lifetime measurements are responsive to the molecular environment of fluorescent molecules, and contribute information concerning the kinetic mechanisms of regulation and photoprotection of the photosynthetic machinery. For example, energy transfer from the excited molecule to an acceptor, and increased NPQ of the excited state both contribute to a decrease of the fluorescence lifetime. Measurements of the lifetime of fluorescence have been used to elucidate the molecular mechanisms implicated in non-photochemical quenching (Gilmore *et al.* 1995, 1998, Briantais *et al.* 1996, Hartel *et al.* 1996, Gilmore and Govindjee 1999, Niyogi 1999).

When photosynthetic organisms are brought from darkness to constant irradiation, fluorescence intensity undergoes large changes with time, known as the Kautsky effect (Kautsky and Hirsch 1931). This is usually referred to as the "fluorescence induction" or the "fluorescence transient". The characteristics of this transient are identified by the acronym OJIPSMT, where O refers to the "constant" minimum fluorescence, J and I refer to the intermediate inflections before the fluorescence reaches its maximum P, S signifies a semi-steady state, M stands for another peak (or maximum), and T is the terminal

steady state (cf. Govindjee 1995, Lazár 1999). The transient reflects mainly the kinetics of electron transfer in PS2, but it is influenced by protonation events, by PS1 activities, and by changes in the absorption cross-section. The integral of the maximum fluorescence *minus* the fluorescence value of the transient curve over time up to the time of the maximum (this integral is called the complementary area) reflects the size of the plastoquinone pool (Malkin and Kok 1966, Murata *et al.* 1966, Lavorel *et al.* 1986, Stirbet *et al.* 1998). These fluorescence changes present complications in carrying out fluorescence lifetime measurements unless the data can be obtained rapidly (as described for the instrument presented here, see Materials and methods).

For reviews on lifetime measurements and their application in photosynthesis research see Moya *et al.* (1986), Holzwarth (1991), Dau (1994), Gilmore and Govindjee (1999), and Agati *et al.* (2000). The lifetime of Chl *a* fluorescence in higher plants has been measured in intact leaves (Berg *et al.* 1997, Morales *et al.* 1999, Agati *et al.* 2000, Gilmore *et al.* 2000), in chloroplasts (Franck *et al.* 1995) and thylakoids (Gilmore *et al.* 1996a,b). In order to determine the fluorescence lifetimes during transitory changes in the overall fluorescence efficiency of Chl *a*, we present a new instrument capable of rapidly acquiring lifetime-resolved fluorescence images of intact plant tissues at the cellular and subcellular level.

Fluorescence lifetime-resolved imaging, FLI, is expected to provide valuable additional information for distinguishing diverse quenching processes that are involved in Chl a^* de-excitation, and for better understanding of how the immediate environment can modify these mechanisms. The versatility of the FLI instrument will be illustrated with several examples. In particular, we show images of leaves of *Zea mays* and *Arabidopsis thaliana*, and single cells of the green alga *Chlamydomonas reinhardtii*.

Materials and methods

Instrumentation: The FLI instrument described here operates by modulating the excitation radiation at high frequencies (HF), and observing the phase delay and demodulation (decrease in the depth of the amplitude modulation) of the fluorescence emission relative to the phase and modulation of the excitation radiation (Fig. 1). These dynamic fluorescence parameters can be related directly to the lifetime of the fluorescence emission (Duschinsky 1933a,b, Spencer and Weber 1969). This is a known method for measuring the fluorescence decay characteristics of a sample in a single channel mode (cuvette type experiment – for a review see Jameson *et al.* 1984). The lifetime determination is carried out in the frequency domain with sinusoidally modulated radiation, rather than directly in the time domain following very short pulses of radiation. In the FLI instrument, the phase delay and the demodulation are determined rapidly and simultaneously at every pixel of the image. Lifetime-resolved measurements are carried out at several ten thousand pixels simultaneously.

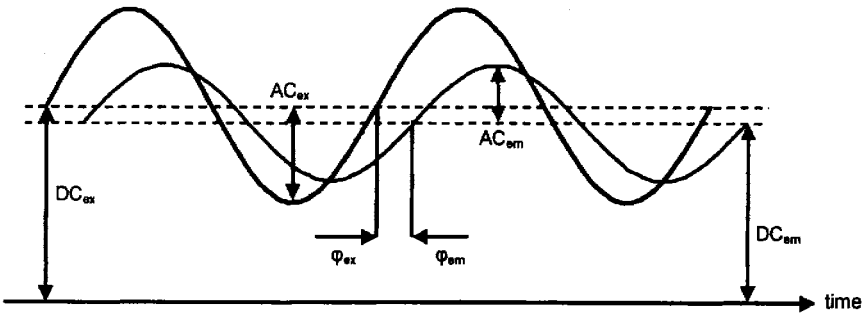

Fig. 1. Frequency domain operation. A fluorophore is excited with intensity modulated excitation radiation of radial frequency ω. The emitted fluorescence signal has the same frequency, but undergoes a phase shift φ and amplitude demodulation M with respect to the excitation radiation depending on the fluorescence lifetimes. This results in two potentially different lifetime estimates τ_{phase} and τ_{mod}, the apparent single lifetimes. AC and DC are the amplitudes of the alternating and direct part of the excitation (ex) or fluorescence emission (em) signal. The modulation depth of the excitation radiation is described by $M_{ex} = AC_{ex}/DC_{ex}$ and of the emission radiation by $M_{em} = AC_{em}/DC_{em}$, respectively. The modulation is then defined as $M = M_{em}/M_{ex}$ and the phase as $\varphi = \varphi_{em} - \varphi_{ex}$. In the case of a mono-exponential decay (a single lifetime component) $M = 1/\sqrt{1+(\omega\tau_{mod})^2}$ and $\varphi = \arctan(\omega\tau_{phase})$ and $\tau_{phase} = \tau_{mod}$, but for more complex lifetime compositions $\tau_{phase} < \tau_{mod}$.

Instrument operation: For the measurements reported in this paper, our frequency domain instrument (Figs. 2 and 3) employs an 80 MHz sinusoidal modulation of the excitation radiation. In order to measure the fluorescence

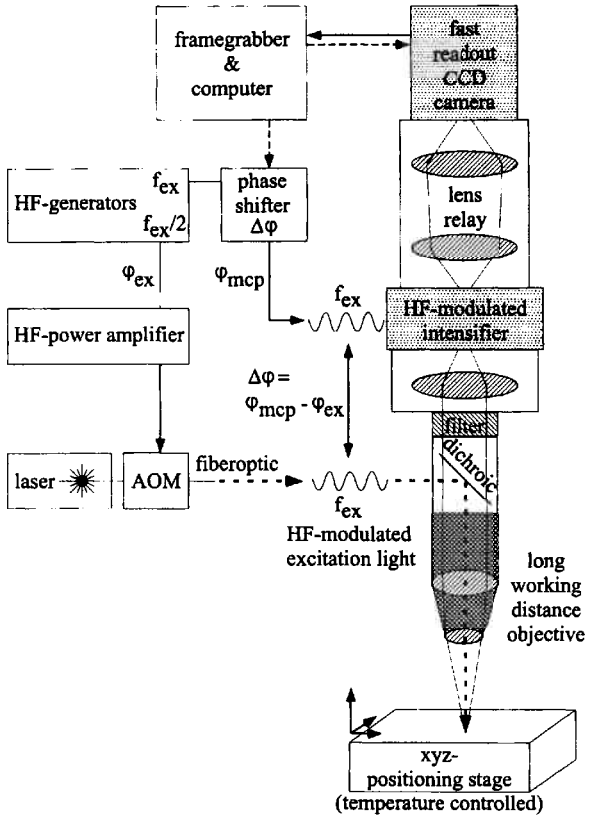

Fig. 2. Scheme of the FLI-instrument. Frequency domain apparatus for lifetime-resolved fluorescence images. Radiation from a continuous wave argon-ion laser is sinusoidally modulated at high frequency (HF) with a standing wave acousto-optical modulator (AOM). Long working-distance objectives (5 to 100 times magnification) are used for irradiating the sample with the modulated radiation. The sample is placed on a temperature controlled xyz-scanning stage; the fluorescence image is projected onto an image intensifier. The cathode voltage of this microchannel plate (MCP) image intensifier is modulated with the identical frequency of the modulated excitation radiation f_{ex} (this constitutes a homodyne mode of operation). The phase of the image intensifier modulation φ_{mcp} differs from the phase of the modulated excitation radiation φ_{ex} by $\Delta\varphi$, which is under computer control. $\Delta\varphi$ is incrementally varied during the measurement. A fast charge coupled device (CCD) camera captures the separate images taken at several incrementally phase-delayed settings, and the acquired images are processed and displayed in real-time on a personal computer (PC).

emission, which is modulated with the same frequency as the excitation radiation, homodyne detection is used. This means that the primary fluorescence detector (the image intensifier) is modulated at the same frequency as the excitation radiation. The output image of the intensifier is focused onto the CCD (charge-coupled-device) detector. The image can be integrated directly at the pixel storage wells of the CCD camera, before transferring the pixel data to the computer. Differences in the lifetime at different pixels correspond both to a difference in amplitude (modulation depth) and to a difference in the phase shift of the modulated emission radiation relative to the excitation radiation. These values can be measured by acquiring images at different phase settings between the excitation radiation and the detector modulation as described below (cf. Clegg *et al.* 1996, Schneider and Clegg 1997). The description presented here is restricted to essential issues important for understanding the operation and analysis; engineering and software details will be published elsewhere.

Instrument design and construction: Figs. 2 and 3 show a scheme and a photograph of our FLI-instrument. Radiation (457, 488, or 514 nm) from an argon-ion laser is sinusoidally modulated by a standing wave acousto-optical modulator (AOM), driven by a HF signal generator. The modulated radiation is coupled into a single mode optical fiber. The sample is placed on a temperature-controlled microscope platform, and can be positioned by an xyz scanning stage. The instrument uses long working distance objectives (5× to 100× magnification; see Appendix). The fluorescence passes through a dichroic mirror and a filter (690±40 nm bandpass for Chl *a* fluorescence). The image is then projected onto a HF-modulated image intensifier. The amplification of the image intensifier is modulated at the same frequency as the excitation radiation. The HF signals driving the AOM and the intensifier are phase-locked. The phase of the HF sinusoidal modulation of the image intensifier relative to the phase of the AOM modulation is computer-controlled by a digital delay-line phase shifter. A CCD camera captures the images at the output of the intensifier, and the images are then read into a computer, processed, and displayed in real-time. A series of incrementally phase-delayed images is acquired, from which the lifetime-resolved information can be calculated. The CCD-camera is a frame transfer camera, which allows rapid image readout (from mapped camera regions) during the acquisition of the next image. To avoid photodamage of samples, a fast shutter is used to turn the radiation on and off at the beginning and end of the acquisition of a complete set of images.

Sixty-six thousand individual pixel measurements are simultaneously acquired at each phase; these are the 300×220 superpixels (2×2 binned camera pixels) of each separate image. Digital Fourier analysis of the consecutive phase-delayed images is performed for each pixel. These calculations with subsequent display of the lifetime images are executed rapidly.

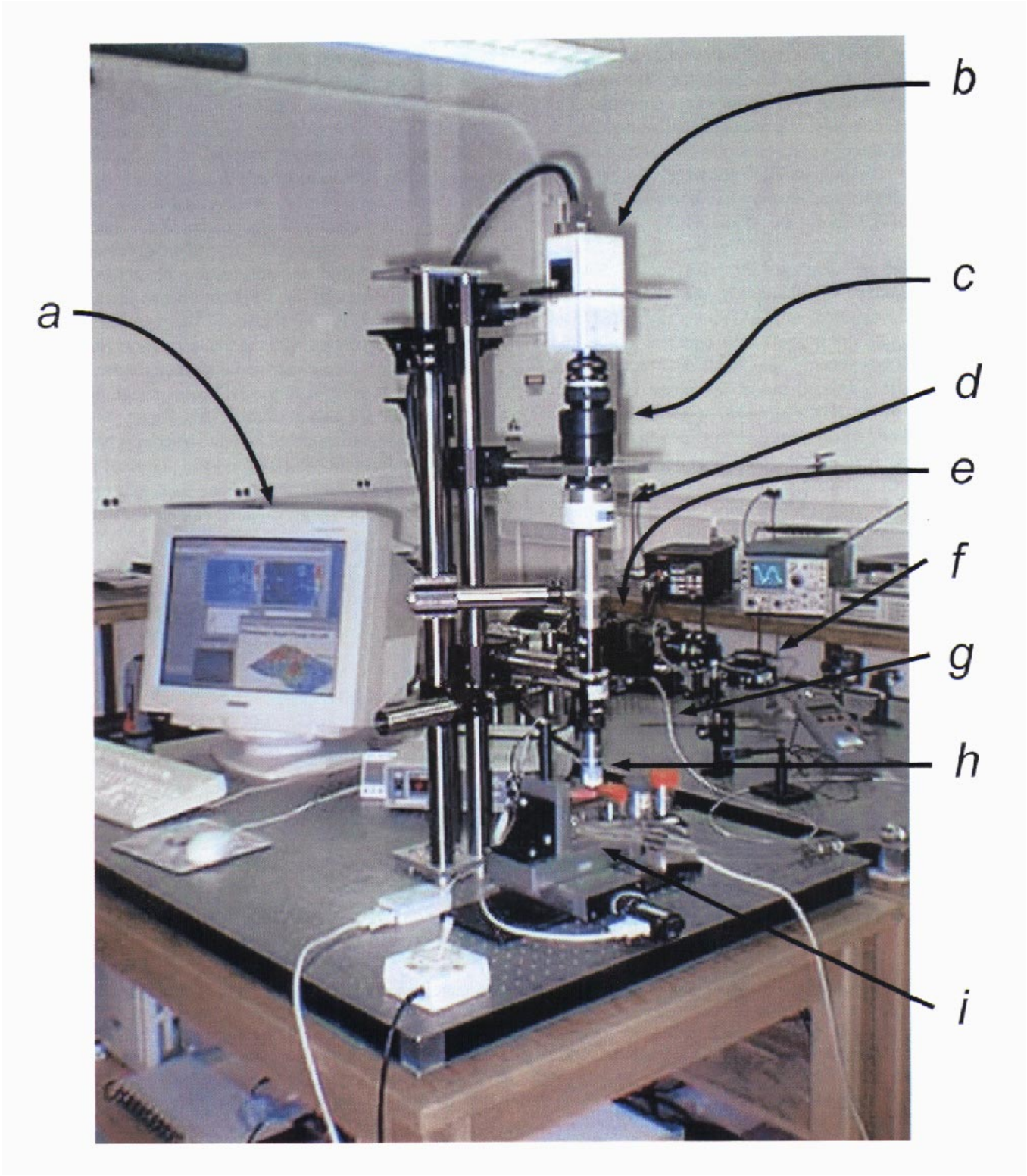

Fig. 3. Photograph of the stage-scanning instrument for fluorescence lifetime-resolved imaging (FLI). The instrument is described in details in the legend of Fig. 2. *a*: Real-time computer display (two and three dimensional lifetime-resolved difference images displayed with 25 Hz). *b*: Fast readout charge coupled device (CCD)-camera. *c*: Relay optics. *d*: High frequency-modulated image intensifier. *e*: Argon-ion laser. *f*: Acousto-optical modulator. *g*: Single mode optical fiber. *h*: Long working distance objective. *i*: Temperature controlled xyz-positioning stage.

A computer controls the instrument. It is equipped with a general purpose interface bus (GPIB) card for controlling the signal generator, a data acquisition card for shifting the phase and controlling the shutter, and a digital frame-grabber for reading the image from the CCD camera into the computer memory. The movement of the xyz-positioning stage is controlled *via* the serial port (*RS 232*) of the computer. The software for control, acquisition, analysis, and display has been developed in *C++* and *LabVIEW 5* for the *Windows NT 4* operating system.

The images are displayed in false colors. Several images are displayed simultaneously: the intensity image, the image of the apparent single lifetimes calculated from phase shift (τ_{phase}), the image of the apparent single lifetimes calculated from demodulation (τ_{mod}), and, depending on the selected mode, the phase and modulation images or the ND image (ND = normalized difference, see below). Histogram displays (number of pixels *vs.* intensities or lifetime characteristics) of all the images and two dimensional histogram displays of τ_{mod} *vs.* τ_{phase} offer fast access to image statistics. These histograms provide a critical monitor for the dynamic range adjustment of the image intensifier. A graph shows the average image intensity at each sequential phase setting. These data are fitted with a sine wave, and the fit is shown together with the residues. This display is especially useful for photosynthetic samples. If one does not choose a region of constant intensity in the fluorescence transient curve, deviation from a sine is clearly discernible in the fit. In particular, with regard to the samples reported in this paper, if the exposure of the sample to radiation before the start of the lifetime measurement (the F_0 to F_P region of the transient; usually about 300 ms – 1 s) is not long enough for the fluorescence intensity to reach its maximum F_P, the sinusoidal fluorescence modulation will be convoluted with the transient curve (Fig. 4).

As an option, three-dimensional surface renderings of the measured intensity with the ND color image mapped onto the surface are also available. This display, which is useful for the visualization of certain structures, has been achieved at video rate (25 Hz) for 164×123 pixel images concurrent with the image acquisition. A manufacturer list of the instrumentation is given in the Appendix.

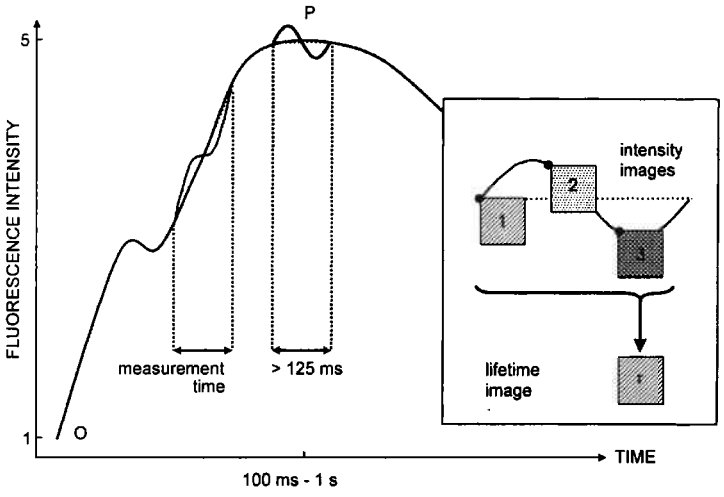

Fig. 4. The fluorescence transient and lifetime measurements. Three or more phase-delayed images (images of the fluorescence intensity with a different incremented phase difference $\Delta\varphi$) are necessary to obtain a fluorescence lifetime image (see *insert*). The lifetime measurements were done at the P-level, where one usually obtains several seconds of constant fluorescence intensity. This allows analysis of the modulated fluorescence emission signal without corrections for additional changes in the intensity, as they occur for example at the rapid intensity increase in the beginning of the fluorescence transient. The minimal necessary measurement time for a lifetime image (3 phase-delayed images of 300×220 superpixel; 2×2 binning) is down to 125 ms in the described setup. Such fast measurement times allow the imaging at the P-level.

Lifetime determination using the Fourier analysis mode (the apparent single fluorescence lifetime at every pixel): To obtain the phase and modulation of the fluorescence signal relative to the phase and modulation of the excitation radiation, the phase between the 80 MHz modulation of the excitation radiation and the detector (image intensifier) is varied in known phase increments. The fluorescence signal is acquired with a good signal-to-noise ratio at each phase setting. The recorded signals are then analyzed by rapid digital Fourier methods and lifetimes for the case of a single lifetime component (the apparent lifetimes τ_{phase} and τ_{mod}) are calculated (Clegg and Schneider 1996, Schneider and Clegg 1997). For this analysis, the measurement of the signal at three different

phases is the minimum requirement for determining a lifetime of fluorescence; however, information about lifetime differences can be obtained rapidly by measuring at only two phases, as discussed in the next section.

The Fourier analysis mode allows lifetime measurements to be performed rapidly (update rate of 0.7 Hz with display of 3 images and histogram analysis). Thus it can be used for screening samples. The signal-to-noise ratio of images of low irradiance can be improved to the desired precision by simply lengthening the measurement time at each phase setting, provided of course that the measurement conditions allow a longer integration. Unless data are acquired at multiple frequencies, the lifetime reported at every pixel is a mean lifetime, averaged in a weighted fashion over the contributing lifetime components. In the case of multiple lifetime components and if only one frequency is used, the apparent single lifetime from the fit of the modulation data is always longer than the apparent single lifetime from the fit of the phase data.

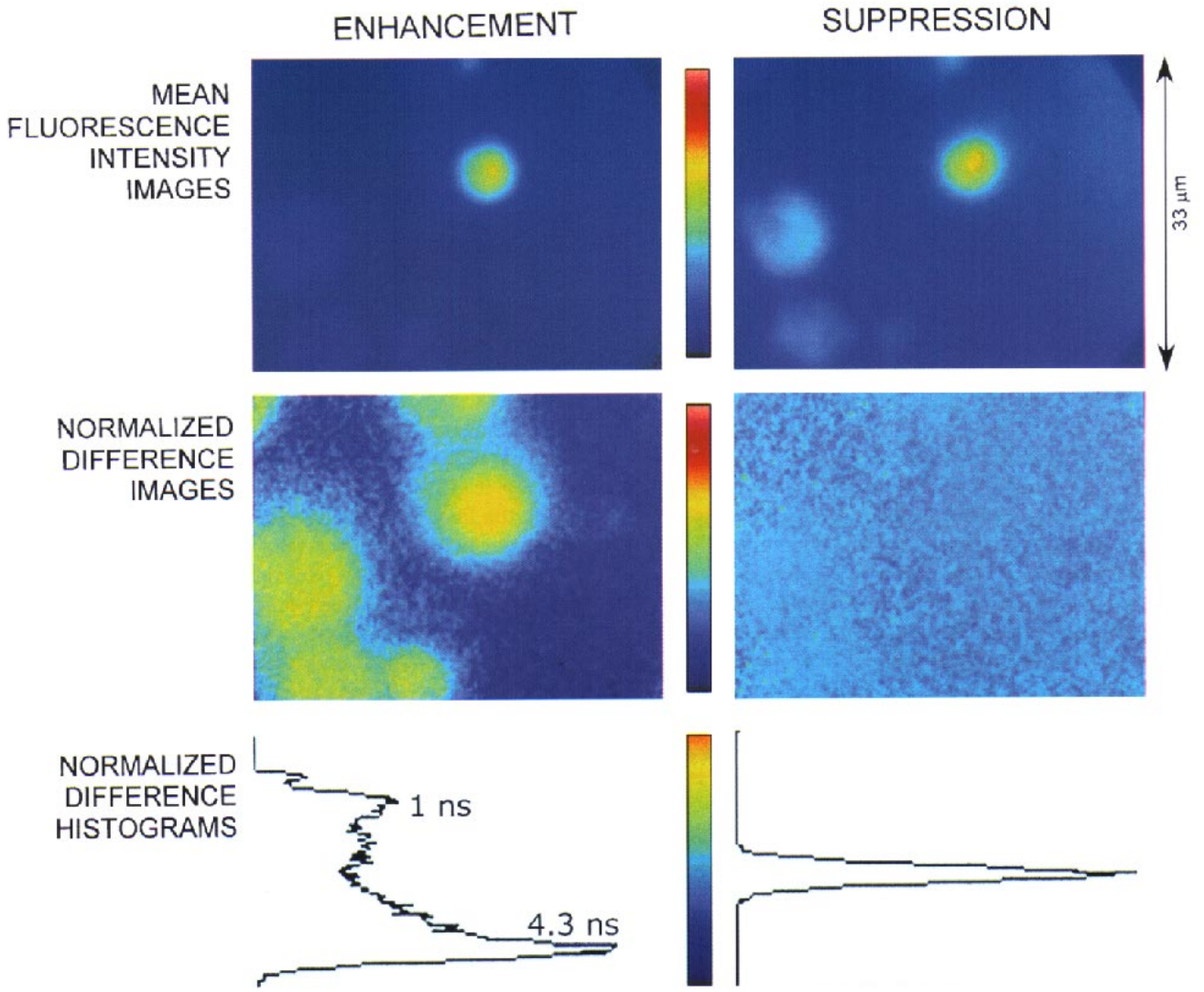

Fig. 5. Enhancement and suppression of spatially separated fluorescence lifetime differences using the Normalized Difference (ND) mode. Displayed are fluorescence intensity and ND images of immobilized cells of green alga *Chlamydomonas reinhardtii* bathed in sulforhodamine 101 solution. The dye, which has a fluorescence lifetime of 4.3 ns, was added to the *Chlamydomonas* suspensions (with 10 % glycerol for immobilization) to demonstrate lifetime contrast (the fluorescence of Chl *a* from *C. reinhardtii* exhibits the short mean lifetime of about 1 ns). *Left panels*: Enhancement of lifetime differences. The short fluorescence lifetime of the alga is seen as *yellow* and the longer lifetime of the background fluorescence from the dye as *dark blue* in the ND image. *Right panels*: Shifting the phase $\Delta\varphi$ of the previous settings by 90° suppresses the differences in the ND-image so that there is no difference between the ND signal from both fluorescence signals (the ND from the fluorescence of both alga and background are displayed as light blue). The scale of all images in this figure is the same.

The Normalized Difference (ND) mode: This mode (Schneider and Clegg 1997) is faster than the mode where the actual lifetime is determined. The ND mode displays lifetime difference images calculated from only two images. The fluorescence emission signals are measured at two phases differing by π, and then the difference of these two images is normalized to the average intensity at every pixel, which is the sum of the two images. The value of this ND at every pixel depends on the lifetime components of fluorescence emitted. This mode is faster because it requires only two phase-delayed images to calculate one lifetime-difference image. For continuous acquisition and analysis the previous π shifted image is reused in the calculation with the phase-delayed image just acquired, yielding one displayed ND-image per measured phase-delayed image. Our system can display the ND-image and its intensity image (328×247 superpixels; 2×2 binning) at video rate (25 Hz) with an integration time of 19 ms for each of the two phase-delayed images. At higher camera binning modes, this process can be speeded up, so that we can measure, analyze, and display at 55 Hz for 164×123 superpixels (4×4 pixel binning) using a 10 ms integration time. The phase settings can be varied interactively, allowing both suppression and enhancement of certain chosen lifetime components. By adjusting the phase settings for this difference mode, the user can visually scan through phase delays that correspond to certain fluorescence lifetimes, and locate positions of the image which have fluorescence components that are greater than, less than, or equal to a particular selected lifetime value. In the ND mode, the actual lifetimes at different pixels are not calculated; but, they are compared. The resulting images can be color-coded to represent specific values (or ranges of values) of the ND. This is a useful option if one is looking for evidence of specific lifetimes in samples with several different fluorescence lifetime components. The phase can be varied while the ND-images are being displayed at video rate; this allows fast screening of samples. However, one must remember that the ND is not an absolute reading, and that one is measuring a complex quantity when one is looking at a sample with multiple components. This is especially important when one is interpreting a ND image taken at only a single phase setting. Observed ND differences in an image always correspond to differences in phase and modulation. But if one does not see any differences at a fixed phase setting it does not imply that there are no differences in phase and modulation. For instance, if two different lifetime components are spatially separated, one can always choose one phase setting, such that these components have identical ND readings (see Fig. 5).

Fluorescence transient and lifetime measurements: For lifetime measurements of fluorescence the data acquisition must take place during defined time periods of irradiation where the fluorescence signal is constant. If the fluorescence intensity changes during the time of the measurement, artifacts will arise. The artifacts are due to distortions of the sine curve (fluorescence *versus* phase delay) in the frequency domain[1]. If the decay characteristics of the fluorescence change during the measurement time, then any measurement of the lifetime must take place in a period of time short compared to these kinetics, or the measurement (no matter whether it takes place in the frequency or time domain) will be affected.

Dark-adapted photosynthetic systems change their Chl fluorescence intensity (fluorescence transient; see Introduction) when irradiated. The fluorescence level of photosynthetic systems increases upon sufficient irradiation to a maximum (F_{max}), 5-10 times the original level F_0, and this usually takes place in time scales ranging from 100 ms up to 1 s. The intensity can increase by a factor of four within 0.2 ms. Under certain conditions the changes in fluorescence intensity of photosynthetic systems directly reflect changes in the lifetime of the fluorescence as discussed in a review by Govindjee (1995).

In the frequency domain (that we use for data acquisition), the fluorescence transient (the Kautsky curve) will be convoluted with the sinusoidal fluorescence emission signal (Fig. 4), and unless the measurement is very short compared to the time of the induction curve, or is made in a region of constant fluorescence, the analysis would also be distorted through this convolution.

Sample preparation and measurements

Leaves of maize (*Zea mays*): The top ends of maize leaves were cut off and mounted on a microscope slide. Water soaked tissue at the cut edge of the leaf prevented it from drying. After focusing on the upper side, the leaf was dark adapted for 5 min and the Chl *a* fluorescence transient curve measured. The transient was measured with the FLI instrument using the fast readout capability of the CCD camera (529 Hz; 32×32 pixel binning). At an irradiance of 100 μmol(photon) m^{-2} s^{-1} at 488 nm, the region of constant maximum fluorescence intensity

[1] Many fluorescence lifetime measurements on photosynthetic systems employ direct time domain techniques (see references in Introduction). It is important to realize that in the time domain, intensity changes during the measurement also give rise to similar artifacts affecting both amplitude and lifetime composition.

during the transient of Chl *a* fluorescence is between 0.5-2.1 s (the "P" level). Therefore, following 5 min of dark adaptation, the sample was irradiated for 600 ms before the lifetime was measured. Twenty phase-delayed images of 100 ms integration time each were acquired (fluorescence intensity changes during this time interval were about 5 %). Between 0.35 and 4 s following the initiation of irradiation, the fluorescence intensity changed by only approximately 10 %. Measurements were performed with 10× objective at 250 μmol(photon) m^{-2} s^{-1}.

Leaves of *Arabidopsis thaliana* were severed at the stem and mounted on a microscope slide. A water-soaked tissue at the cut end of the leaf prevented them from drying. After focusing on the upper side, the leaf was dark adapted for 5 min and the fluorescence transient was measured. The region of maximum constant intensity of Chl *a* fluorescence was found between 0.6-3.0 s following the beginning of irradiation with 100 μmol(photon) m^{-2} s^{-1} at 488 nm (5× objective). Even up to 4 s the fluorescence intensities were still within one standard deviation of the plateau value. Therefore, the sample was irradiated for 600 ms after 5 min of dark adaptation before the lifetime was measured. Thirty phase-delayed images each integrated for 100 ms were acquired (fluorescence intensity changes during this time interval were only 2.5 %). We imaged areas along the main vein of the leaf. The water soaked tissue was removed in order to dehydrate the leaf, and the measurements were repeated after several hours.

Cells of *Chlamydomonas reinhardtii* were grown photoheterotrophically at 100 μmol(photon) m^{-2} s^{-1} in Tris-acetate phosphate (TAP) medium (pH 7) (Harris 1989) at 25 °C. The protocol described bellow was followed at room temperature. The sample in the microscope was kept at 20 °C with a temperature-controlled stage. Prior to the fluorescence lifetime measurements, the cell suspension was dark adapted for 5 min. When needed, 3-(3,4-dichlorophenyl)-1,1-dimethylurea (DCMU, diuron; *Sigma,* St. Louis, MO, USA) was added in darkness to the cell suspension (10 μM final concentration), followed by a 5 min incubation in the dark. Using a mild vacuum, cells were deposited on a nitrocellulose filter (pore size 1.2 μm; *Millipore,* Bedford, MA, USA) that had been soaked previously in minimum High Salt (HS) medium (Harris 1989). This was done to avoid out-of-focus movement of the cells under the microscope due to the water uptake of the filter. The filter was then covered with minimum HS medium (pH 7) and a cover slip. The cells were irradiated in the microscope (100× objective) at low irradiance [15 μmol(photon) m^{-2} s^{-1}] for focussing. After that the cells were irradiated briefly with 2300 μmol (photon) m^{-2} s^{-1} to adjust the image intensifier gain for an optimal dynamic range of the camera. This was followed by dark adaptation of the cells for 5 min. The experimental conditions for the fluorescence lifetime measurements were as follows. The 457 nm line of the argon-ion laser, modulated at 80.652 MHz, was used for irradiation. The wavelength of the measured fluorescence was 690±40 nm (bandpass filter *Omega XF70/690DF40*).

The excitation irradiance was 2300 μmol(photon) m^{-2} s^{-1}. The cells were pre-irradiated for 350 ms before 36 phase-delayed images, each averaged for 100 ms, were acquired, so that the total irradiation time of the measurement was 3.6 s. This time range allowed measurement within the constant region of the transient (at the "P" level).

Results and discussion

Not many examples of lifetime-resolved images of Chl-fluorescence have been presented in the literature. A lifetime-resolved difference image of a leaf taken under irradiation-adapted conditions has been published as an example of lifetime component suppression (Gadella *et al.* 1993, Clegg *et al.* 1994). Sanders *et al.* (1996) published fluorescence lifetime-resolved images of Chl *b* in polymer matrices. French (1996) showed a lifetime-resolved image (integrated for 300 s) of the two chloroplasts of two *Spirogyra* cells, which display differences in the lifetime of Chl fluorescence. König *et al.* (1998) presented ultrafast time-gated fluorescence images of Chl *a* of a microalga in an optical multitrap. From measurements at different time-delays they could determine the lifetime of fluorescence.

We present here lifetime-resolved images of the Chl *a*-fluorescence of leaves for the first time. The images of the apparent lifetimes calculated from phase and modulation could be acquired within the short time interval of maximum and constant fluorescence at the P-level of the transient curve. We present three examples to demonstrate the use of FLI for studying photosynthetic processes, and for studying stress-induced changes in the photosynthetic performance. First, we show differences in the lifetime of Chl *a* fluorescence between bundle sheath cells and mesophyll cells of maize (*Z. mays*). The results can be understood in terms of differences between these cell types. Secondly, we show that dehydration induces spatially heterogeneous changes in the lifetimes of fluorescence from mesophyll cells on both sides of the main vein of leaves of *A. thaliana*. As a third example, we show how FLI can be used for studying non-photochemical quenching (NPQ) in photosynthesis. We show lifetime-resolved images of single cells of wild type (WT) and the zeaxanthin accumulating mutant NPQ2 (Niyogi *et al.* 1997) of *C. reinhardtii*. These images

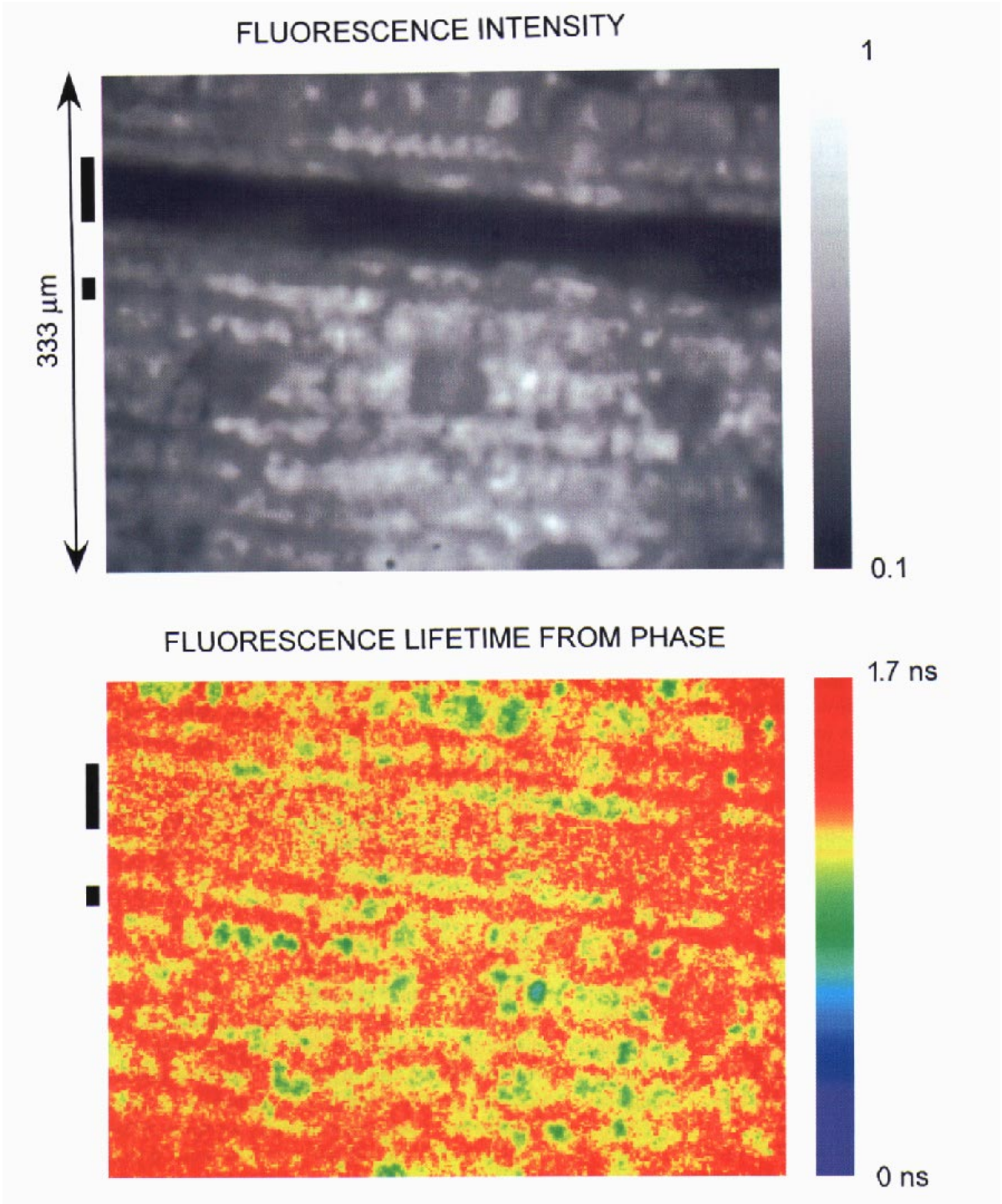

Fig. 6. Images of intensities and lifetimes of Chl *a* fluorescence from the adaxial leaf surface of a young maize (*Zea mays*) leaf. Displayed are images of the Chl *a* fluorescence intensity (*top*) and the apparent single lifetime from the phase (*bottom*) of the upper side of a young maize leaf. One sees a single lateral vein and the surrounding mesophyll cells (with defocused stomatal complexes). There are differences in the apparent lifetimes between the fluorescence from the center of the mesophyll cells (τ_{phase} = 1.0±0.1 ns; *yellow*) and the fluorescence (of about 1.4 times lower intensity) from the rim of the cells (τ_{phase} = 1.3±0.1 ns; *red*). Measurement conditions: excitation wavelength, 488 nm; emission wavelength, 690±40 nm; modulation frequency, 80.652 MHz; objective magnification, ×10; irradiance, 250 µmol(photon) m^{-2} s^{-1}. After 5 min dark adaptation, the sample was irradiated for 350 ms, after which 36 images (each image with a different incremented phase difference Δφ) were acquired at 100 ms per image resulting in a total illumination time of 3.6 s. The *two black bars* on the left side of the images help in comparing the two images. The scale of all images in this figure is the same.

display remarkable differences between the lifetimes of Chl *a* fluorescence from WT and NPQ2 mutant cells.

Some technical aspects are discussed under "Practical factors influencing interpretations of thick samples, such as leaves".

Lifetime-resolved images of the Chl *a* fluorescence of maize leaves: Figs. 6 and 7 show fluorescence lifetime images of the upper side of maize leaves determined from the phase. The fluorescence lifetime images from the modulation (not displayed here) show the same pattern. Measurements (results given in Table 1, but images not shown) similar to those in Fig. 6 were done with irradiance at 250 μmol(photon) m^{-2} s^{-1} with a pre-irradiation for 600 ms. Twenty phase-delayed images were taken at 100 ms each, resulting in a total irradiation time of 2 s. Under this radiation exposure (longer pre-exposure and shorter measurement time than in Fig. 6), measurements in the transient region of constant and maximum (P-level) intensity could be carried out.

In the fluorescence intensity image of Fig. 6, a lateral vein (40-50 μm wide) and the adjacent tissue are seen. The Chl *a* fluorescence from the top layer directly under the epidermis is from mesophyll cells. The defocused low intensity fluorescence spots (about 45×45 μm) are from the guard cells of the stomata. The fluorescence intensity from the center of the mesophyll cells is higher (by a factor of 1.4) than the fluorescence emanating from closer to the cell wall. The apparent single fluorescence lifetimes in the center of the mesophyll cells are shorter than in areas of the cell closer to the cell wall. The explanation for this lifetime difference is not clear. Chloroplasts, which are strongly absorbing, surround the vacuoles. The centers of mesophyll cells are relatively transparent. The excitation radiation penetrates through the transparent vacuole in the center, which is devoid of chloroplasts. Therefore, the Chl *a* fluorescence seen at the center of the mesophyll cells originates from chloroplasts lying deeper below the surface (below the vacuoles). The shorter lifetime in this region could imply that the cells lying deeper below the leaf surface actually have chloroplasts that are inherently different from the chloroplasts surrounding the vacuoles in the upper layers. However, assuming that the chloroplasts show no differences, which one would expect for the same kind of cells, the shorter lifetime might be due to a lower irradiance of the excitation radiation in this lower layer, which leads to lower transient fluorescence, and therefore shorter lifetimes. The fluorescence yield and lifetime of Chl *a* fluorescence of PS2 depend on the irradiance. Fewer PS2 centers are closed (*i.e.*, P is lower) in deeper (shaded) chloroplasts than in upper (fully irradiated) chloroplasts. Further experiments are needed to answer the questions raised. But the differences are significant and reproducible.

Veins are framed by bundle sheath cells. In the left panel of Fig. 7, a smaller vein parallel to a larger lateral vein can be seen. The fluorescence of the bundle sheath cells has a shorter apparent single lifetime than the mesophyll cells that are between the two bundles (see Table 1). This is even more perceptible in the right panel of Fig. 7, where the focal plane of the objective is farther below the surface of the leaf (defocusing slightly the top layer of mesophyll cells). That the lifetime of the Chl *a* fluorescence from bundle sheath cells is shorter than the one from mesophyll cells is in agreement with what is known about the distribution of the two photosystems, with their different fluorescence yields, in these two types of cells. Bundle sheath cells are richer in PS1 than mesophyll cells (Bazzaz and Govindjee 1973, Horváth *et al.* 1978, Edwards *et al.* 2001). PS1 contributes a short lifetime component of about 0.1 ns, the intensity of which is constant during the transient induction curve. The intensities and lifetimes of all components of PS2 are dependent on the irradiation; the long lifetime reaches 2 ns at F_{max} (cf. Holzwarth 1991).

The lifetime calculated from the phase data (τ_{phase}) is always identical to the lifetime calculated from the amplitude modulation data (τ_{mod}), if the fluorescence signal is derived from a single lifetime component. A difference in the two lifetimes indicates multiple lifetime components. Because we observe differences in τ_{phase} and τ_{mod}, our data can be rationalized by assuming two major lifetime components. In general one cannot resolve more than one component with a single frequency measurement [however, see Verveer *et al.* (2000) for special cases where global analyses can give two lifetimes from single frequency measurements]. Nevertheless, if we assume to have a two lifetime component system and that the short lifetime component is $\tau_1 = 0.1$ ns (the usual main lifetime component of PS1), then τ_2 and its fractional intensity f_2 can be calculated from the measured apparent lifetimes (Weber 1981). For discussions of Weber's algorithm in the context of imaging applications, see Gadella *et al.* (1994) and Jameson (2001). The results of this analysis are given in Table 1 together with the average lifetime calculated from τ_1 and τ_2. One recognizes that the average lifetime of the bundle sheath cells for this two-lifetime component system is slightly shorter than the lifetime of the mesophyll cells, just as found when fitting the data to a single lifetime. We caution that the measurements described here are not exact determinations of the fluorescence lifetime of bundle sheath cells because the fluorescence signal that we are ascribing to them is composed of fluorescence from both mesophyll cells and bundle sheath cells. The fluorescence from mesophyll cells, which are lying above the bundle sheath cells, contributes a longer lifetime component to the overall fluorescence from the area of the image corresponding to the bundle sheath cells. A precise

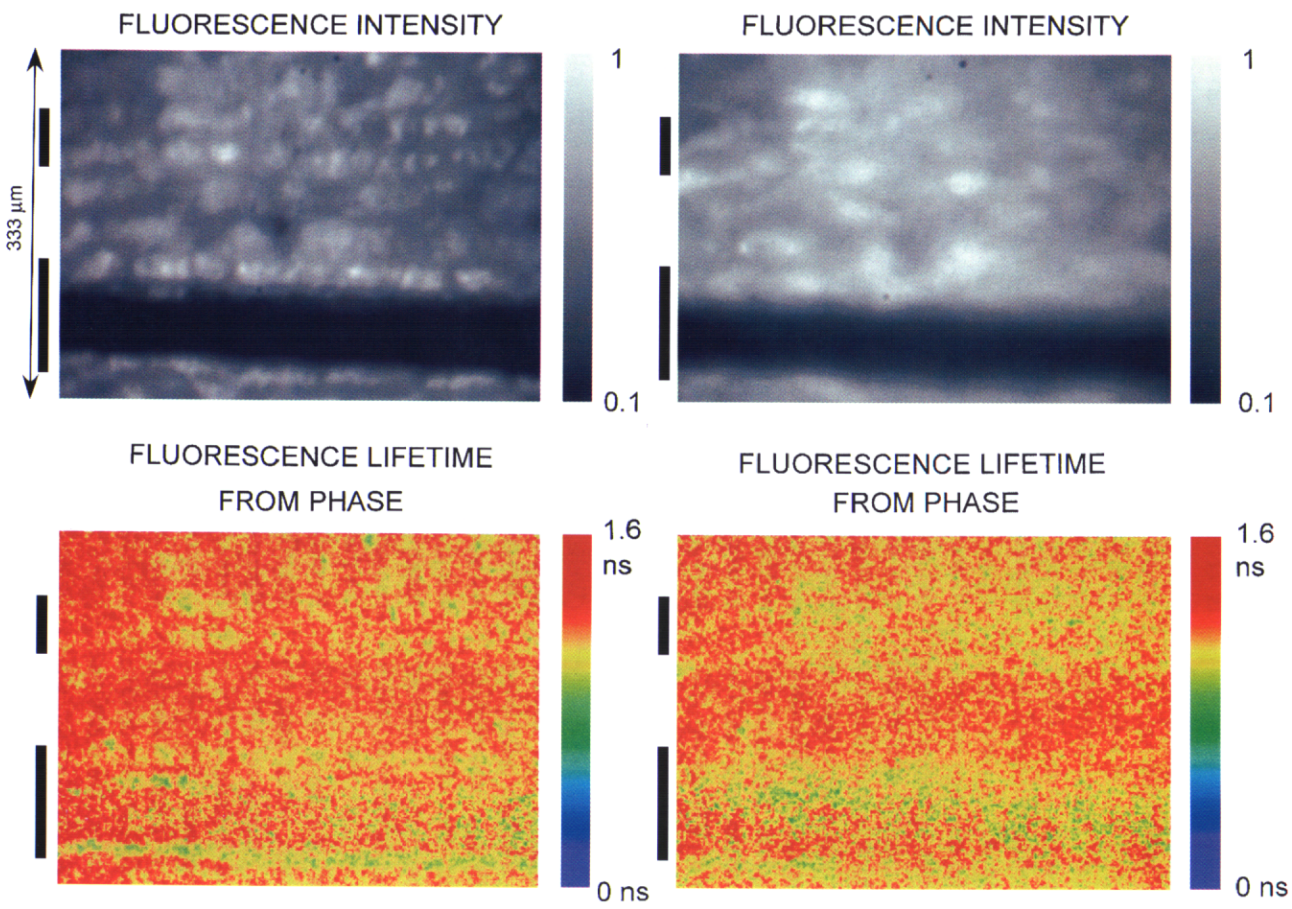

Fig. 7. Images of intensities and lifetimes of Chl *a* fluorescence from the adaxial surface of a mature maize (*Zea mays*) leaf. *Left panels*: Chl *a* fluorescence intensity (*top*) and lifetime-resolved (*bottom*) images of the upper side of a mature maize leaf. As in Fig. 6, a lateral vein and the surrounding mesophyll cells (with defocused stomatal complexes) can be seen. A second smaller vein is lying parallel to the larger lateral vein. Differences are displayed in the apparent single fluorescence lifetimes between bundle sheath cells and mesophyll cells. The bundle sheath cells surround the veins and are seen as two framing lines of cells on the borders of each vein. They display the shorter apparent single lifetime of τ_{phase} = 1.0±0.1 (*yellow*) in comparison to the mesophyll cells (τ_{phase} = 1.1±0.1; *red*). Measurement conditions: excitation wavelength, 488 nm; emission wavelength, 690±40 nm; modulation frequency, 80.652 MHz; objective magnification, ×10; irradiance, 250 µmol(photon) m^{-2} s^{-1}. After 5 min dark adaptation, the sample was irradiated for 500 ms, after which 36 images (each image with a different incremented phase difference Δφ) were acquired at 100 ms per image resulting in a total irradiation time of 3.6 s. *Right panels*: The same imaged area as shown in the left panel (under the same measurement conditions), but with the focal plane of the objective moved farther below the surface of the leaf, which slightly defocuses the top layer of mesophyll cells. The mesophyll cells can be seen as a *red band* of longer apparent fluorescence lifetime in contrast to the shorter fluorescence lifetime (*yellow*) of the bundle sheath cells on the sides of the two veins. Stomatal complexes are lying in the epidermis and, due to focusing on the mesophyll cells, are only visible as defocused areas of low fluorescence intensity on top of the mesophyll cells between the two veins. The *two black bars* on the left side of the images mark the ordinate position of the two veins surrounded by bundle sheath cells and help in comparing the images. The scale of all images in this figure is the same.

determination of the fluorescence lifetimes in images of bundle sheath cells in whole leaf samples requires confocal or point spread function deconvolution lifetime-resolved imaging methods.

Lifetime-resolved image of the Chl *a* fluorescence of a leaf of *A. thaliana*

Effect of dehydration: Fig. 8 shows a ND image of *A. thaliana* after dehydration. Additional measurements (images of the lifetimes are not shown, but results are presented below) were carried out with leaves that were dark-adapted for 5 min. The samples were then irradiated for 600 ms, after which 30 images (each image with a different incremented phase difference $\Delta\varphi$) were acquired at 100 ms per image resulting in a total irradiation time of 3.0 s. This time range allowed the measurements in the constant region of the P-level fluorescence under the irradiance of 100 μmol m^{-2} s^{-1} at 488 nm. These images displayed similar lifetime patterns as seen by the lifetime differences in Fig. 8. In all cases the fluorescence lifetimes at the rim of the mesophyll cells are the longest, $\tau_{phase} = \tau_{mod} = 1.9\pm0.2$ ns (corresponding to the yellow/red regions in the ND image of Fig. 8). The identical phase and modulation lifetimes indicate that a single lifetime component describes the fluorescence decay from this measurement. The centers of mesophyll cells above the main vein show the shorter time $\tau_{phase} = 1.6\pm0.2$ ns and $\tau_{mod} = 1.8\pm0.2$ ns (corresponding to blue regions in the ND image of Fig. 8) independent of the time of dehydration over several hours. Immediately after detachment of the leaf from the plant, the centers of mesophyll cells on both sides of the main vein show the same lifetime as the centers of mesophyll cells above the main vein. However, after several hours following detachment, the τ_{phase} at the centers of the mesophyll cells on both sides of the main vein changes to $\tau_{phase} = \tau_{mod} = 1.8\pm0.2$ ns (corresponding to green regions in the ND image of Fig. 8). This change accentuates the main vein as seen in Fig. 8, which was not the case before dehydration.

The mesophyll cells of *A. thaliana* leaves (Fig. 8) show the same heterogeneous lifetime pattern as seen in the images of the maize leaves. The centers of the mesophyll cells show higher fluorescence intensity with a 300 ps shorter apparent single lifetime than at the rim of the cells (see discussion of the images of the maize leaves). However, no other differences in the lifetimes of Chl *a* fluorescence could be detected in undetached leaves. The heterogeneous lifetime pattern of the mesophyll cells is identical above and at both sides of the main vein (images not shown). Detachment of leaves and dehydration over several hours leads to small changes in the fluorescence lifetime of the mesophyll cell centers on the sides of the main vein. This heterogeneity in the lifetime image accentuates the mesophyll cells above the main vein as shown in Fig. 8. The apparent single lifetime calculated from the phase of the fluorescence from the center of these cells changed on the average only 150 ps.

In general, one might expect a decrease in the average lifetime after dehydration due to increased non-photochemical quenching (Cerovic *et al.* 1996) and not the observed slight increase. The complex events taking place during dehydration make it impossible without additional experiments to speculate on the underlying processes responsible for the observed changes. However, this example demonstrates that interesting processes take place under stress that can be observed by FLI, which are not observable by intensity measurements alone. FLI measurements provide additional valuable parameters for comparing the behavior of plants under different states of stress.

Comments on measurements of leaves: Leaves from different plants show distinctive lifetime patterns of the Chl *a* fluorescence originating from their mesophyll cells. The heterogeneous lifetime pattern of the mesophyll cells displayed in Figs. 6 and 8, where the fluorescence of higher intensity from the centers displays a shorter lifetime than from the rim of the cells (see also discussion of maize images above), was generally observed from leaves of different plants. These structures though visible in the intensity image, were often easier to distinguish in the lifetime images. In addition to this mesophyll structure, the venation structures could often be observed.

Practical factors influencing interpretations of thick samples, such as leaves: By imaging the lifetime-resolved fluorescence signals (as seen in Figs. 6 to 8) differences in photosynthesis can be related to specific locations in the structure of the leaves. However, some practical factors concerning the optical properties of leaves must be considered. Different wavelengths of radiation have different penetration depths, and the contribution from lower lying material depends on the wavelength and the objectives used. We have shown mainly the fluorescence from sub-epidermal layers of the leaves. Objectives with high magnification focus radiation into small volumes, and the fluorescence radiation emanates mainly from the focal region. Objectives with low magnification have a greater depth of focus (see Appendix for a description of the objectives), and will collect fluorescence from thicker sections. Factors such as different depths of focus must be taken into account when interpreting images of samples with a thickness greater than the depth of focus.

In some cases we show ND-images that are averages of many rapidly acquired ND-images. Differences in these averaged images could result from true life-time differences in the F_P region of constant

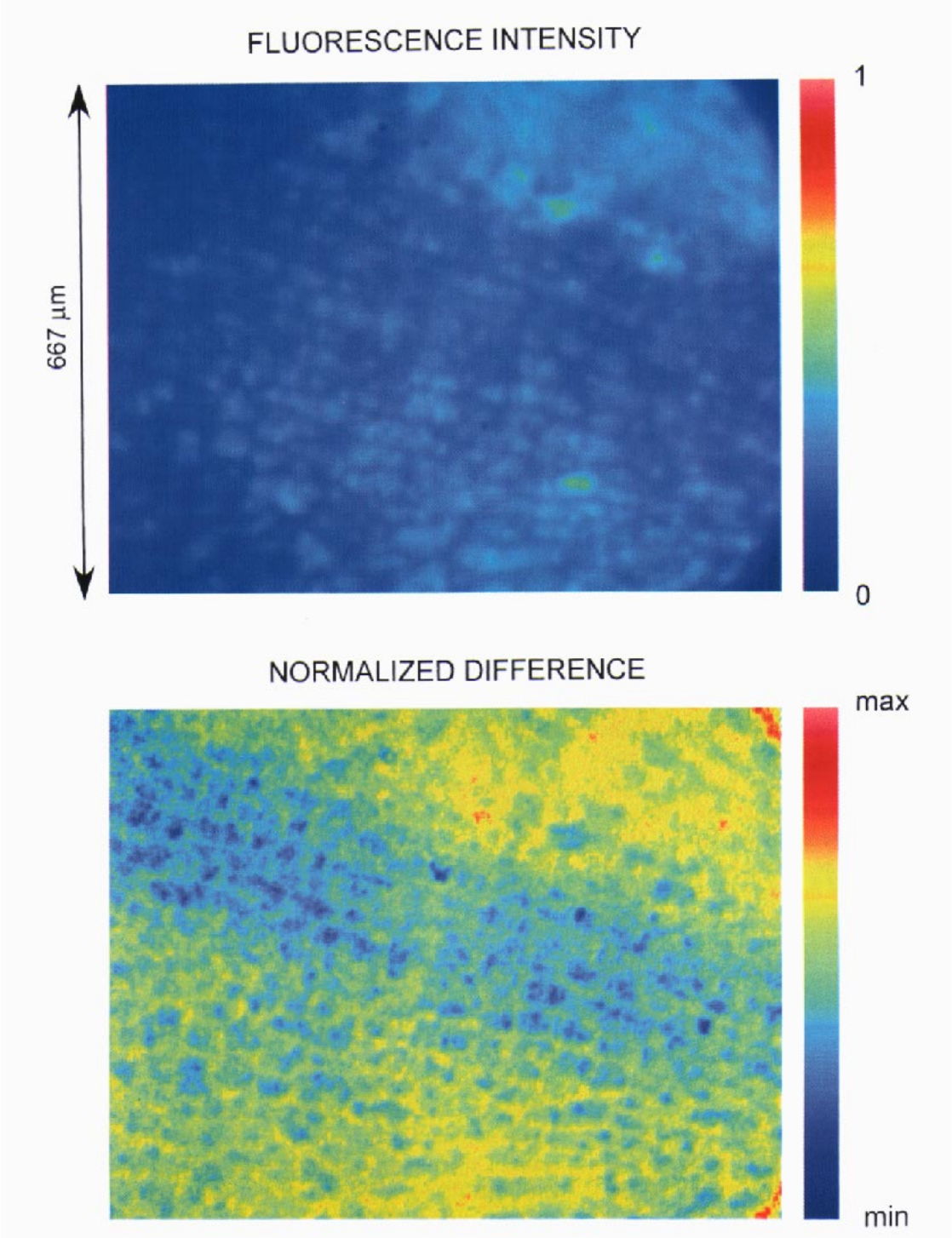

Fig. 8. Images of the Chl *a* fluorescence from a leaf of *Arabidopsis thaliana* (adaxial) following dehydration. Chl *a* fluorescence intensity (*top*) and lifetime-resolved (*bottom*) difference images (normalized difference, ND, image) of the main vein on the upper side of a leaf of *A. thaliana*, measured after 1 h and 15 min dehydration time following leaf detachment. The fluorescence from the mesophyll cells displays lifetime differences between their centers (high intensity, shorter lifetime) and their rim (lower intensity, longer lifetime). Lifetime differences are also seen between mesophyll cells above the main vein and mesophyll cells on both sides of the vein. This accentuates the main vein in this lifetime-resolved image. These differences could not be observed immediately following detachment (homogeneous images, except for the general differences in the lifetimes from the mesophyll cells) but only after a longer dehydration period. Measurement conditions were: excitation wavelength, 488 nm; emission wavelength, 690±40 nm; modulation frequency, 80.652 MHz; objective magnification, ×5; irradiance, 100 µmol(photon) m^{-2} s^{-1}. After pre-irradiation the ND-images and the intensity images were integrated for several seconds. The images were acquired at a rate of 15 Hz. The scale of all images in this figure is the same.

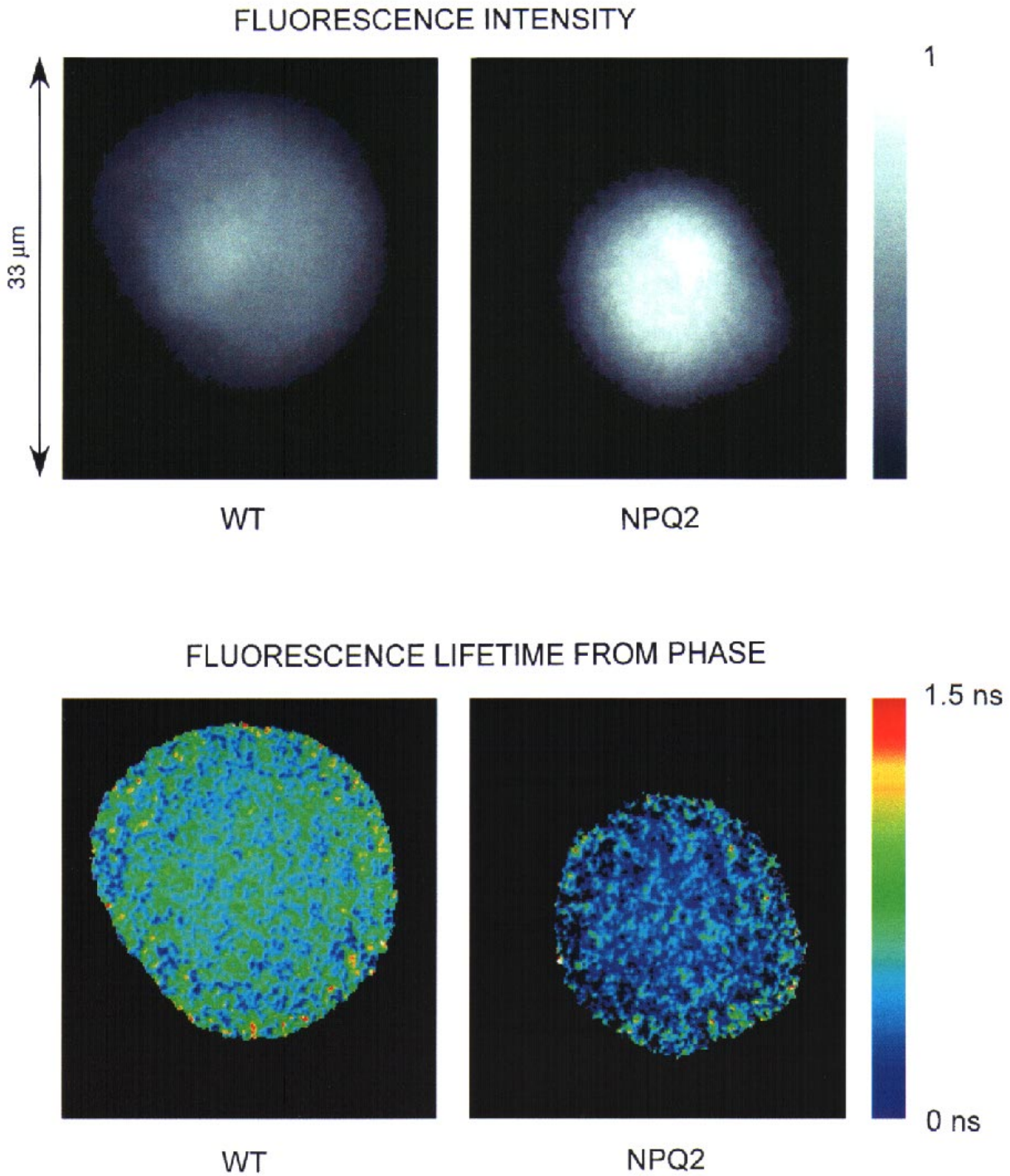

Fig. 9. Images of the Chl *a* fluorescence from single cells of *Chlamydomonas reinhardtii*: Comparison of a WT cell with a NPQ2 mutant cell. Intensity (*top*) and lifetime-resolved (*bottom*) images of the Chl *a* fluorescence of two single cells of wild type (WT) and non-photochemical quenching (NPQ) mutant NPQ2 of the alga *C. reinhardtii*. The NPQ2 mutant accumulates zeaxanthin (Niyogi *et al.* 1997). Both cells were treated with 10 µM DCMU (see Materials and methods). The WT cell, which has a 1.5 times lower maximum fluorescence intensity compared to the NPQ2 cell shown here, displays the longer lifetime of τ_{phase} = 0.6±0.2 ns (*green*). NPQ2 shows the shorter time of τ_{phase} = 0.3±0.2 ns (*blue*). The apparent lifetime calculated from the modulation is τ_{mod} = 1.0±0.4 ns for both cells (τ_{mod} images not shown). Measurement conditions: excitation wavelength, 457 nm; emission wavelength, 690±40 nm; modulation frequency, 80.652 MHz; objective magnification, ×100; irradiance, 2 300 µmol(photon) m^{-2} s^{-1}. After 5 min dark adaptation the sample was irradiated for 350 ms, after which 36 images (each image with a different incremented phase difference $\Delta\varphi$) were acquired at 100 ms per image resulting in a total irradiation time of 3.6 s (this time range allowed the measurement to be made in the constant region of the transient, the P-level fluorescence, under this irradiance). The scale of all images in this figure is the same.

fluorescence intensity. However, if the lifetimes are changing during the averaging process (as they do during certain periods of the transient), then the apparent ND values would be different if the transients have different kinetics at separate locations. Therefore, in all cases we have made additional measurements at the relative maximum fluorescence F_P, which were used to determine the reported lifetimes.

Table 1. Apparent single lifetimes τ_{phase} and τ_{mod} from lifetime-resolved images of maize leaves at F_P with an irradiance of 250 μmol(photon) m^{-2} s^{-1}, extracted by local histogram analysis of image regions. The second lifetime component τ_2 and its fractional intensity f_2 were calculated as described by Weber (1981) for an assumed two-lifetime component system where the first lifetime component is $\tau_1 = 0.1$ ns. For this case the average lifetime $<\tau> = f_1 \tau_1 + f_2 \tau_2$ is also given. The values in columns 3 and 4 refer to the yellow and red areas of Fig. 7. The values for columns 1 and 2 refer to measurements taken with a different series of cells than shown in Fig. 6, as described in the text. However, the lifetimes shown in columns 1 and 2 correspond to similar cellular locations as shown in the red and yellow areas of the cells in Fig. 6.

Model	Mesophyll cells (rim) (Fig. 6, *red*)	Mesophyll cells (center) (Fig. 6, *yellow*)	Bundle sheath cells (Fig. 7, *yellow*)	Mesophyll cells (Fig. 7, *red*)
Measured apparent single lifetimes of Chl *a* fluorescence	$\tau_{phase} = 1.7 \pm 0.2$ ns $\tau_{mod} = 2.0 \pm 0.2$ ns	$\tau_{phase} = 1.4 \pm 0.2$ ns $\tau_{mod} = 1.7 \pm 0.2$ ns	$\tau_{phase} = 1.0 \pm 0.1$ ns $\tau_{mod} = 1.1 \pm 0.2$ ns	$\tau_{phase} = 1.1 \pm 0.1$ ns $\tau_{mod} = 1.2 \pm 0.2$ ns
For a two lifetime component system with $\tau_1 = 0.1$ ns	$\tau_2 = 2.0$ ns ($f_2 = 91$ %) $<\tau> = 1.9$ ns	$\tau_2 = 1.7$ ns ($f_2 = 87$ %) $<\tau> = 1.5$ ns	$\tau_2 = 1.1$ ns ($f_2 = 91$ %) $<\tau> = 1.0$ ns	$\tau_2 = 1.3$ ns ($f_2 = 92$ %) $<\tau> = 1.2$ ns

Lifetime-resolved images of the Chl *a* fluorescence of single cells of *C. reinhardtii*, wild type (WT) and the NPQ2 mutant: Photoprotection of PS2 by non-photochemical quenching (NPQ) of Chl *a* fluorescence is correlated with the conversion of violaxanthin to zeaxanthin *via* antheraxanthin during the so-called xanthophyll cycle (Demmig-Adams *et al.* 1996). For models of NPQ, see Crofts and Yerkes (1994) and Gilmore *et al.* (1995, 1998). At normal irradiance, energy is channeled very efficiently by Förster-transfer from the Light-Harvesting-Complex (LHC2b) and/or from other minor Chl-protein complexes to the reaction center of PS2 (PS2RC). Under intense irradiation, lumen acidification leads to the enzymatic conversion of violaxanthin to antheraxanthin, then to zeaxanthin, and finally to structural changes in the minor Chl-protein complexes, *e.g.*, CP29, and in all likelihood the *psbS* gene product (Li *et al.* 2000). These changes favor the binding of zeaxanthin. Zeaxanthin is believed to be a better quencher than violaxanthin, although the lowest excited singlet states heve been reported to be similar (Frank *et al.* 2000). Thus, conformational changes may also be involved in the phenomenon. The mutant NPQ2 (Niyogi *et al.* 1997) accumulates zeaxanthin. Fig. 9 shows the image of a single cell of this mutant and that of a wild type cell of *C. reinhardtii*. The particular WT cell used here had a 1.5× lower maximum fluorescence intensity compared to the NPQ2 cell. This demonstrates the general problem of interpreting fluorescence intensity signals in microscopy, where the local fluorophore concentrations are not known. When comparing the average fluorescence intensities from cell suspensions of identical Chl concentrations, NPQ2 has a lower fluorescence intensity than the WT. However, the measurement of fluorescence lifetime is independent of such local concentration variations. Thus, the observed differences in fluorescence intensity shown here must be due to differences in Chl concentration of the two cells. Cells of NPQ2 show in general a shorter apparent lifetime calculated from the phase. The complete analysis of these measurements will be presented elsewhere. The shorter τ_{phase} can be explained with a higher fraction of a short lifetime component in NPQ2. Zeaxanthin (accumulated in NPQ2) therefore quenches the Chl *a* fluorescence of PS2 in *C. reinhardtii* by decreasing the quantum yield of Chl *a* fluorescence and not only by decreasing the absorption cross section of the pigment bed (static quenching). This conclusion could only have been obtained by measuring the fluorescence lifetimes. Förster transfer from Chl *a* to zeaxanthin could explain this decrease in the lifetime of Chl *a* in the NPQ2 mutant, especially because NPQ2 and WT have similar PS1/PS2 ratios and comparable antenna sizes based on similar Chl *a*/*b* ratios and comparable β-carotene contents (Jahns *et al.* 2000).

Concluding remarks: Fluorescence imaging techniques are usually based on the measurement of fluorescence intensity. This signal is often ambiguous because it is influenced by numerous factors. In particular, changes in the absorption cross section of the fluorescent PS2 leads to changes in the fluorescence intensity, but not in the fluorescence lifetimes. Simultaneous fluorescence intensity and lifetime measurements (*i.e.*, FLI) provide additional information for understanding the functioning of the photosynthetic apparatus. We have developed a scheme using FLI for obtaining lifetime-resolved images that is applicable during the Chl *a* fluorescence transient curve. By making measurements at the "P" level in an

interval of constant fluorescence intensity, errors in the lifetime-resolved image measurement, that can occur if the measurement is made during large transient fluorescence intensity changes, are avoided. We believe that FLI will provide important clues for understanding the functioning of several biological systems.

References

Agati, G., Cerovic, Z.G., Moya, I.: The effect of decreasing temperature up to chilling values on the *in vivo* F685/F735 chlorophyll fluorescence ratio in *Phaseolus vulgaris* and *Pisum sativum*: The role of the photosystem I contribution to the 735 nm fluorescence band. - Photochem. Photobiol. **72**: 75-84, 2000.

Bazzaz, M.B., Govindjee: Photochemical properties of mesophyll and bundle sheath chloroplasts of maize. - Plant Physiol. **52**: 257-262, 1973.

Berg, D., Maier, K., Otteken, D., Terjung, F.: Picosecond fluorescence decay studies on water-stressed pea leaves: energy transfer and quenching processes in Photosystem 2. - Photosynthetica **34**: 97-106, 1997.

Briantais, J.-M., Dacosta, J., Goulas, Y., Ducruet, J.-M., Moya, I.: Heat stress induces in leaves an increase of the minimum level of chlorophyll fluorescence, F_0: A time-resolved analysis. - Photosynth. Res. **48**: 189-196, 1996.

Buschmann, C., Lichtenthaler, H.K.: Principles and characteristics of multi-colour fluorescence imaging of plants. - J. Plant Physiol. **152**: 297-314, 1998.

Byrdin, M., Rimke, I., Schlodder, E., Stehlik, D., Roelofs, T.A.: Decay kinetics and quantum yields of fluorescence in photosystem I from *Synechococcus elongatus* with P700 in the reduced and oxidized state: Are the kinetics of excited state decay trap-limited or transfer-limited? - Biophys. J. **79**: 992-1007, 2000.

Cerovic, Z.G., Goulas, Y., Gorbunov, M., Briantais, J.M., Camenen, L., Moya, I.: Fluorosensing of water stress in plants - diurnal changes of the mean lifetime and yield of chlorophyll fluorescence, measured simultaneously and at distance with a tau-LIDAR and a modified PAM-fluorimeter, in maize, sugar beet, and *Kalanchoe*. - Remote Sens. Environ. **58**: 311-321, 1996.

Ciscato, M.: Development of a Fluorescence Imaging System for the Quality Assessment of Fruits and Vegetables. - PhD. Thesis. Limburgs Universitair Centrum (LUC), Diepenbeek 2000.

Clegg, R.M., Gadella, T.W.J., Jovin, T.M.: Lifetime-resolved fluorescence imaging. - Proc. SPIE **2137**: 105-118, 1994.

Clegg, R.M., Schneider, P.C.: Fluorescence Lifetime-resolved Imaging Microscopy: A general description of the lifetime-resolved imaging measurements. - In: Slavik, J. (ed.): Fluorescence Microscopy and Fluorescent Probes. Pp. 15-33. Plenum Press, New York 1996.

Clegg, R.M., Schneider, P.C., Jovin, T.M.: Fluorescence Lifetime-resolved Imaging Microscopy. - In: Verga Scheggi, A.M., Martellucci, S., Chester, A.N., Pratesi, R. (ed.): Biomedical Optical Instrumentation and Laser-Assisted Biotechnology. Vol. 325. Pp. 143-156. Kluwer Academic Publ., Dordrecht - Boston - London 1996.

Crofts, A.R., Yerkes, C.T.: A molecular mechanism for q_E-quenching. - FEBS Lett. **352**: 265-270, 1994.

Daley, P.F.: Chlorophyll fluorescence analysis and imaging in plant stress and disease. - Can. J. Plant Pathol. **17**: 167-173, 1995.

Dau, H.: Molecular mechanisms and quantitative models of variable photosystem II fluorescence. - Photochem. Photobiol. **60**: 1-23, 1994.

DeEll, J.R., Toivonen, P.M.A.: Chlorophyll fluorescence as a nondestructive indicator of broccoli quality during storage in modified-atmosphere packaging. - HortScience **35**: 256-259, 2000.

Demmig-Adams, B., Gilmore, A.M., Adams, W.W., III: *In vivo* function of carotenoids in higher plants. - FASEB J. **10**: 403-412, 1996.

Duschinsky, F.: Der zeitliche Intensitätsverlauf von intermittierend angeregter Resonanzstrahlung. - Z. Phys. **81**: 7-22, 1933a.

Duschinsky, F.: Eine allgemeine Theorie der zur Messung sehr kurzer Leuchtdauern dienenden Versuchsanordnungen (Fluorometer); A general theory of the instruments for the measurement of very short after-glows (Fluorometer). - Z. Phys. **81**: 23-42, 1933b.

Edwards, G.E., Furbank, R.T., Hatch, M.D., Osmond, C.B.: What does it take to be C4? Lessons from the evolution of C4 photosynthesis. - Plant Physiol. **125**: 46-49, 2001.

Franck, F., Schoefs, B., Barthélemy, X., Myśliwa-Kurdziel, B., Strzałka, K., Popovic, R.: Protection of native chlorophyll(ide) forms and of photosystem II against photodamage during early stages of chloroplast differentiation. - Acta Physiol. Plant. **17**: 123-132, 1995.

Frank, H.A., Bautista, J.A., Josue, J.S., Young, A.J.: Mechanism of nonphotochemical quenching in green plants: Energies of the lowest excited singlet states of violaxanthin and zeaxanthin. - Biochemistry **39**: 2831-2837, 2000.

French, T.: The Development of Fluorescence Lifetime Imaging and an Application in Immunology. - PhD. Thesis. University of Illinois at Urbana-Champaign, Urbana 1996.

Gadella, T.W.J., Jr.: Fluorescence Lifetime Imaging Microscopy (FLIM): Instrumentation and applications. - In: Mason, W.T. (ed.): Fluorescent and Luminescent Probes for Biological Activity. Pp. 467-479. Academic Press, San Diego 1999.

Gadella, T.W.J., Jr., Clegg, R.M., Jovin, T.M.: Fluorescence lifetime imaging microscopy: pixel-by-pixel analysis of phase-modulation data. - Bioimaging **2**: 139-159, 1994.

Gadella, T.W.J., Jr., Jovin, T.M., Clegg, R.M.: Fluorescence lifetime imaging microscopy (FLIM): Spatial resolution of microstructures on the nanosecond time scale. - Biophys. Chem. **48**: 221-239, 1993.

Genty, B., Meyer, S.: Quantitative mapping of leaf photosynthesis using chlorophyll fluorescence imaging. - Aust. J. Plant Physiol. **22**: 277-284, 1995.

Gilmore, A.M., Govindjee: How higher plants respond to excess light: Energy dissipation in photosystem II. - In:

Singhal, G.S., Renger, G., Sopory, S., Irrgang, K.D., Govindjee (ed.): Concepts in Photobiology. Pp. 513-548. Narosa Publ. House, Delhi - Madras - Bombay - Calcuta - London; Kluwer Academic Publ., Boston - Dordrecht - London 1999.

Gilmore, A.M., Hazlett, T.L., Debrunner, P.G., Govindjee: Comparative time-resolved photosystem II chlorophyll *a* fluorescence analyses reveal distinctive differences between photoinhibitory reaction center damage and xanthophyll cycle-dependent energy dissipation. - Photochem. Photobiol. **64**: 552-563, 1996a.

Gilmore, A.M., Hazlett, T.L., Debrunner, P.G., Govindjee: Photosystem II chlorophyll *a* fluorescence lifetimes and intensity are independent of the antenna size differences between barley wild-type and *chlorina* mutants. Photochemical quenching and xanthophyll cycle-dependent nonphotochemical quenching of fluorescence. - Photosynth. Res. **48**: 171-187, 1996b.

Gilmore, A.M., Hazlett, T.L., Govindjee: Xanthophyll cycle-dependent quenching of photosystem II chlorophyll *a* fluorescence: Formation of a quenching complex with a short fluorescence lifetime. - Proc. nat. Acad. Sci. USA **92**: 2273-2277, 1995.

Gilmore, A.M., Itoh, S., Govindjee: Global spectral-kinetic analysis of room temperature chlorophyll *a* fluorescence from light-harvesting antenna mutants of barley. - Phil. Trans. roy. Soc. London **B 355:** 1371-1384, 2000.

Gilmore, A.M., Shinkarev, V.P., Hazlett, T.L., Govindjee: Quantitative analysis of the effects of intrathylakoid pH and xanthophyll cycle pigments on chlorophyll *a* fluorescence lifetime distributions and intensity in thylakoids. - Biochemistry **37**: 13582-13593, 1998.

Govindjee: Sixty-three years since Kautsky: Chlorophyll *a* fluorescence. - Aust. J. Plant Physiol. **22**: 131-160, 1995.

Govindjee, Amesz, J., Fork, D.C. (ed.): Light Emission by Plants and Bacteria. - Academic Press, Orlando - San Diego - New York - Austin - Boston - London - Sydney - Tokyo - Toronto 1986.

Harris, E.H.: The *Chlamydomonas* Sourcebook. - Academic Press, San Diego - New York - Berkeley - Boston - London - Sydney - Tokyo - Toronto 1989.

Hartel, H., Lokstein, H., Grimm, B., Rank, B.: Kinetic studies on the xanthophyll cycle in barley leaves. Influence of antenna size and relations to nonphotochemical chlorophyll fluorescence quenching. - Plant Physiol. **110**: 471-482, 1996.

Holzwarth, A.R.: Excited-state kinetics in chlorophyll systems and its relationship to the functional organization of the photosystems. - In: Scheer, H. (ed.): Chlorophylls. Pp. 1125-1151. CRC Press, Boca Raton - Ann Arbor - Boston - London 1991.

Horváth, G., Droppa, M., Mustárdy, L., Faludi-Dániel, Á.: Functional characteristics of intact chloroplasts isolated from mesophyll protoplasts and bundle sheath cells of maize. - Planta **141**: 239-244, 1978.

Jahns, P., Depka, B., Trebst, A.: Xanthophyll cycle mutants from *Chlamydomonas reinhardtii* indicate a role for zeaxanthin in the D1 protein turnover. - Plant Physiol. Biochem. **38**: 371-376, 2000.

Jalink, H., van der Schoor, R., Frandas, A., van Pijlen, J.G., Bino, R.J.: Chlorophyll fluorescence of *Brassica oleracea* seeds as a non-destructive marker for seed maturity and seed performance. - Seed Sci. Res. **8**: 437-443, 1998.

Jameson, D.M.: The Seminal Contributions of Gregorio Weber to Modern Fluorescence Spectroscopy. Methods and Applications of Fluorescence Spectroscopy. - Springer-Verlag, Heidelberg 2001.

Jameson, D.M., Gratton, E., Hall, R.D.: The measurement and analysis of heterogeneous emissions by multifrequency phase and modulation fluorometry. - Appl. Spectrosc. Rev. **20**: 55-106, 1984.

Karukstis, K.K.: Chlorophyll fluorescence as a physiological probe of the photosynthetic apparatus. - In: Scheer, H. (ed.): Chlorophylls. Pp. 769-795. CRC Press, Boca Raton - Ann Arbor - Boston - London 1991.

Kautsky, H., Hirsch, A.: Neue Versuche zur Kohlensäure-assimilation. - Naturwissenschaften **19**: 964, 1931.

König, K., Boehme, S., Leclerc, N., Ahuja, R.: Time-gated autofluorescence microscopy of motile green microalga in an optical trap. - Cell. mol. Biol. **44**: 763-770, 1998.

Kramer, D.M., Crofts, A.R.: Control and measurement of photosynthetic electron transport *in vivo*. - In: Baker, N.R. (ed.): Photosynthesis and the Environment. Pp. 25-66. Kluwer Academic Publ., Dordrecht - Boston -London 1996.

Lavorel, J., Breton, J., Lutz, M.: Methodological principles of measurement of light emitted by photosynthetic systems. - In: Govindjee, Amesz, J., Fork, D.C. (ed.): Light Emission by Plants and Bacteria. Pp. 57-98. Academic Press, Orlando - San Diego - New York - Austin - Boston - London - Sydney - Tokyo - Toronto 1986.

Lazár, D.: Chlorophyll *a* fluorescence induction. - Biochim. biophysica Acta **1412**: 1-28, 1999.

Li, X.P., Björkman, O., Shih, C., Grossman, A.R., Rosenquist, M., Jansson, S., Niyogi, K.K.: A pigment-binding protein essential for regulation of photosynthetic light harvesting. - Nature **403**: 391-395, 2000.

Malkin, S., Kok, B.: Fluorescence induction studies in isolated chloroplast. I. Number of components involved in the reaction and quantum yields. - Biochim. biophys. Acta **126**: 413-432, 1966.

Mazza, C.A., Boccalandro, H.E., Giordano, C.V., Battista, D., Scopel, A.L., Ballare, C.L.: Functional significance and induction by solar radiation of ultraviolet-absorbing sunscreens in field-grown soybean crops. - Plant Physiol. **122**: 117-125, 2000.

Morales, F., Belkhodja, R., Goulas, Y., Abadia, J., Moya, I.: Remote and near-contact chlorophyll fluorescence during photosynthetic induction in iron-deficient sugar beet leaves. - Remote Sens. Environ. **69**: 170-178, 1999.

Moya, I., Sebban, P., Haehnel, W.: Lifetime of excited states and quantum yield of chlorophyll *a* fluorescence *in vivo*. - In: Govindjee, Amesz, J., Fork, D.C. (ed.): Light Emission by Plants and Bacteria. Pp. 161-190. Academic Press, Orlando - San Diego - New York - Austin - Boston - London - Sydney - Tokyo - Toronto 1986.

Murata, N., Nishimura, M., Takamiya, A.: Fluorescence of chlorophyll in photosynthetic systems. II. Induction of fluorescence in isolated spinach chloroplasts. - Biochim. biophys. Acta **120**: 23-33, 1966.

Niyogi, K.K.: Photoprotection revisited: Genetic and molecular approaches. - Annu. Rev. Plant Physiol. Plant mol. Biol. **50**: 333-359, 1999.

Niyogi, K.K., Björkman, O., Grossman, A.R.: *Chlamydomonas*

xanthophyll cycle mutants identified by video imaging of chlorophyll fluorescence quenching. - Plant Cell **9**: 1369-1380, 1997.

Oxborough, K., Baker, N.R.: An instrument capable of imaging chlorophyll *a* fluorescence from intact leaves at very low irradiance and at cellular and subcellular levels of organization. - Plant Cell Environ. **20**: 1473-1483, 1997.

Papageorgiou, G.C.: The photosynthesis of cyanobacteria (blue bacteria) from the perspective of signal analysis of chlorophyll *a* fluorescence. - J. sci. ind. Res. **55**: 596-617, 1996.

Samson, G., Prášil, O., Yaakoubd, B.: Photochemical and thermal phases of chlorophyll *a* fluorescence. - Photosynthetica **37**: 163-182, 1999.

Sanders, R., Van Zandvoort, M.A.M.J., Draaijer, A., Levine, Y.K., Gerritsen, H.C.: Confocal fluorescence lifetime imaging of chlorophyll molecules in polymer matrices. - Photochem. Photobiol. **64**: 817-820, 1996.

Schneider, P.C., Clegg, R.M.: Rapid acquisition, analysis, and display of fluorescence lifetime-resolved images for real-time applications. - Rev. sci. Instrum. **68**: 4107-4119, 1997.

Scholes, J.D., Rolfe, S.A.: Photosynthesis in localised regions of oat leaves infected with crown rust (*Puccinia coronata*). Quantitative imaging of chlorophyll fluorescence. - Planta **199**: 573-582, 1996.

Spencer, R.D., Weber, G.: Measurement of subnanosecond fluorescence lifetimes with a cross-correlation phase fluorometer. - Ann. New York Acad. Sci. **158**: 361-376, 1969.

Stirbet, A., Govindjee, Strasser, B.J., Strasser, R.J.: Chlorophyll *a* fluorescence induction in higher plants: Modelling and numerical simulation. - J. theor. Biol. **193**: 131-151, 1998.

Verveer, P.J., Squire, A., Bastiaens, P.I.H.: Global analysis of fluorescence lifetime imaging microscopy data. - Biophys. J. **78**: 2127-2137, 2000.

Wang, X.F., Periasamy, A., Herman, B., Coleman, D.M.: Fluorescence lifetime imaging microscopy (FLIM): instrumentation and applications. - Crit. Rev. anal. Chem. **23**: 369-395, 1992.

Weber, G.: Resolution of the fluorescence lifetimes in a heterogeneous system by phase and modulation measurements. - J. phys. Chem. **85**: 949-953, 1981.

Appendix

List of the instrumentation:

-AOM (20, 40, 80, 100 MHz radiation modulation): acousto-optic standing wave modulator *SWM-102AE1-1, SWM-202AE1-1, SWM-804*, acousto-optic mode locker *SFM-502F1-1* (all: *IntraAction*, Bellwood, IL, USA).
-CCD-camera (cooled fast scan multi format with 10 bit fast scan mode): *C4880/81* (*Hamamatsu Photonics*, Hamamatsu City; Japan).
-Computer: *Intel Pentium III* 550 MHz Processor; 256 MB RAM; *Oxygen GVX1 OpenGL* accelerator graphics card (*3Dlabs*, Sunnyvale, CA, USA); general purpose interface bus (GPIB) PCI card (*National Instruments*, Austin, TX, USA); *6025E DAQ* data acquisition PCI card (*National Instruments*, Austin, TX, USA); EDT PCI-DV digital video camera interface card (framegrabber) (*Engineering Design Team EDT*, Beaverton, OR, USA).
-Digital delay line phase shifter (20, 40, 80 MHz; 0.7° (9 bit) phase resolution): *DP-2-9-20-77, DP-2-9-40-77, DP-2-9-80-77* (*Lorch Microwave*, Salisbury, MD, USA).
-Filters and mirror: laser line filters *XL05* (457 nm), *XL06* (488 nm), XL07 (515 nm) with blocker *B5/B6*, dichroic *XF27/550DCLPO2*, fluorescence emission *XF70/690DF40* (*Omega Optical*, Brattleboro, VT, USA).
-Image intensifier (HF-modulated): *C5825* (*Hamamatsu Photonics*, Hamamatsu City, Japan).
-Laser: multi-line argon-ion *2213-150 MLYVW* (*Uniphase*, San Jose, CA, USA).
-Linear positioning stage: *PI-M 100* series (*M155.11; M125.10*) (*Physik Instrumente*, Waldbronn, Germany).
-Objectives: *Mitutoyo M Plan Apo* 5× (NA 0.14; WDist. 3.4 cm; DF 14 μm), 10× (NA 0.28; WDist. 3.35 cm; DF 3.5 μm), 50× (NA 0.55; WDist. 1.3 cm; DF 0.9 μm), 100× (NA 0.70; WDist. 0.6 cm; DF 0.6 μm) (*MTI*, Aurora, IL, USA).
-Radio frequency (RF)-power amplifier: *ENI 603L* (3 W linear) (*ENI*, Rochester, NY, USA).
-Shutter: *Uniblitz LS2Z2* (*Vincent Associates*, Rochester, NY, USA).
-Signal generators: *HP-8657A* (*Hewlett Packard*, Palo Alto, CA, USA); *PTS 500* (*Programmed Test Sources PTS*, Littleton, MA, USA).
-Single mode fiber and couplers: *Kineflex-M* single mode fiber delivery system FDS-*D-P-1-S-458/514-0.65-FCP* with connectorised optics *FDS-OP/D-458/514-FC-0.65* and coupler *Kinematix-P* (all: *PointSource*, Winchester, Hampshire, England).
-Software: *Windows NT 4 Workstation* (*Microsoft*, Redmond, WA, USA); *LabVIEW 5.1* (*National Instruments*, Austin, TX, USA); *Visual C++ 6* (*Microsoft*, Redmond, WA, USA).
-Water bath: *RTE-140* (*Neslab Instruments*, Newington, NH, USA).